Journal of Magnetic Resonance 298 (2019) 115–126

Contents lists available at ScienceDirect

Journal of Magnetic Resonance

journal homepage: www.elsevier.com/locate/jmr

Enhancing sensitivity of Double Electron-Electron Resonance (DEER) by using Relaxation-Optimized Acquisition Length Distribution (RELOAD) scheme

Sergey Milikisiyants [a], Maxim A. Voinov [a], Antonin Marek [a], Morteza Jafarabadi [a], Jing Liu [b], Rong Han [b], Shenlin Wang [b], Alex I. Smirnov [b,*]

[a] Department of Chemistry, North Carolina State University, 2620 Yarbrough Drive, Raleigh, NC 27695, USA
[b] Beijing Nuclear Magnetic Resonance Center and College of Chemistry and Molecular Engineering, Peking University, 5 Yiheyuan Road, Haidian, Beijing 100871, People's Republic of China

ARTICLE INFO

Article history:
Received 7 September 2018
Revised 2 December 2018
Accepted 4 December 2018
Available online 5 December 2018

Keywords:
PELDOR
DEER
EPR
Spin-labeling
Dipolar spectroscopy
Distance measurements

ABSTRACT

Over the past decades pulsed electron-electron double resonance (PELDOR), often called double electron-electron resonance (DEER), became one of the major spectroscopic tools for measurements of nanometer-scale distances and distance distributions in non-crystalline biological and chemical systems. The method is based on detecting the amplitude of the primary (3-pulse DEER) or refocused (4-pulse DEER) spin echo for the so-called "observer" spins when the other spins coupled to the former by a dipolar interaction are flipped by a "pump" pulse at another EPR frequency. While the timing of the pump pulse is varied in steps, the positions of the observer pulses are typically fixed. For such a detection scheme the total length of the observer pulse train and the electron spin memory time determine the amplitude of the detected echo signal. Usually, the distance range considerations in DEER experiments dictate the total length of the observer pulse train to exceed the phase memory time by a factor of few and this leads to a dramatic loss of the signal-to-noise ratio (*SNR*). While the acquisition of the DEER signal seems to be irrational under such conditions, it is currently the preferred way to conduct DEER because of an effective filtering out of all other unwanted interactions. Here we propose a novel albeit simple approach to improve DEER sensitivity and decrease data acquisition time by introducing the signal acquisition scheme based on ***REL***axation ***O***ptimized ***A***cquisition (Length) ***D***istribution (DEER-RELOAD). In DEER-RELOAD the dipolar phase evolution signal is acquired in multiple segments in which the observer pulses are fixed at the positions to optimize *SNR* just for that specific segment. The length of the segment is chosen to maximize the signal acquisition efficiency according the phase relaxation properties of the spin system. The total DEER trace is then obtained by "stitching" the multiple segments into a one continuous trace. The utility of the DEER-RELOAD acquisition scheme has been demonstrated on an example of the standard 4-pulse DEER sequence applied to two membrane protein complexes labeled with nitroxides. While theoretical gains from the DEER-RELOAD scheme increase with the number of stitched segments, in practice, even dividing the acquisition of the DEER trace into two segments may improve SNR by a factor of >3, as it has been demonstrated for one of these two membrane proteins.

1. Introduction

Nanometer distance measurements by pulsed EPR are based on detection of dipole-dipole interactions between unpaired electronic spins, thus, justifying Pulsed Dipolar Spectroscopy (PDS) as the general name for this method. During the past two decades PDS evolved into a versatile and a widely applicable tool for structure determination of biomacromolecules, macromolecular complexes, and other non-crystalline materials [1–4]. Modern PDS largely relies on two experimental implementations of the method that employ pulses at either (*i*) single or (*ii*) two different EPR frequencies. The main example of the former is provided by the Double Quantum Coherence (DQC) experiment [5–7] while the latter are usually based on 3- or 4-pulse schemes and are called interchangeably Pulsed Electron-Electron Double Resonance (PELDOR) or Double Electron-Electron Resonance (DEER) [8–10]. While either of these methods works well for the two paramagnetic centers with similar spin relaxation properties and relatively narrow EPR spectra such as nitroxide and trityl radicals, another pulse

* Corresponding author.
E-mail address: Alex_Smirnov@ncsu.edu (A.I. Smirnov).

https://doi.org/10.1016/j.jmr.2018.12.004
1090-7807/

EPR experiment - Relaxation Induced Dipolar Modulations Enhancement (RIDME) [11–13] - was shown to be particularly useful if one of the paramagnetic centers is fast relaxing [14] and/or has broad spectral features [15]. Recently, a modification of the RIDME sequence that includes a second frequency pulse and takes an advantage of the ultra-wide excitation band achieved with a long chirp pulse has been also proposed as an alternative to both DEER/PELDOR and DQC [16]. Other notable PDS methods include single-frequency techniques for refocusing, such as SIFTER [17] and "2 + 1" pulse train [18] as well as more recently introduced laser-induced magnetic dipolar spectroscopy (LaserIMD) [19].

Among all the PDS methods described up to this date in the literature, the 4-pulse DEER introduced almost 20 years ago [10] remains the most widely utilized EPR experiment for structure determination of biological nano-objects [20]. The popularity of the 4-pulse DEER is owned by a combination of several features: (*i*) the method selectively measures inter-electron distances while efficiently filtering out (suppressing) all the unwanted interactions; (*ii*) the experimental signal is free of dead-time artifacts, thus, allowing for more accurate measurements of distance distributions; (*iii*) the pulse sequence could be readily implemented using commercial pulse EPR spectrometers; (*iv*) experimental DEER signals are virtually free of the artifacts whereas nearly all other alternative methods described in the literature require rather tedious signal post-processing.

Typically, the key factor limiting the DEER sensitivity and/or distance range is the electronic spin phase memory time, T_m, which is insufficiently long even at cryogenic temperatures. This problem is especially severe for spin-labeled integral membrane proteins because the phase relaxation mechanism is often dominated by magnetic interactions with protons of the lipid acyl chains as well as those the methyl groups abundant in proteins and is known to persist down to very low temperatures [21,22]. For this reason, even with improved sensitivity of Q-band (35 GHz) pulsed EPR instrumentation many 4-pulse DEER experiments with membrane proteins and, particularly, their oligomeric complexes, still require days of data averaging [23]. Thus, further improving DEER sensitivity has been one of the outmost goals of the researchers in the field for many years. These efforts primarily proceeded in three directions: (*i*) increasing magnetic field (frequency) of the DEER experiment above X-band, (*ii*) increasing the excitation bandwidth of the microwave pulses, and (*iii*) decreasing the phase memory loss via dynamic decoupling.

One particularly fruitful avenue for EPR instrumentation development was the use of high power microwave amplifiers for generating pulses above conventional X-band (9 GHz) frequency. Such a technology dramatically improved both absolute and concentration sensitivity of pulsed EPR experiments including PDS [24–28]. Recent advances in digital arbitrary waveform generators (AWGs) made possible to implement shaped and/or chirped broadband pulses in Fourier transform microwave spectroscopy and pulsed EPR [29–33]. DEER has strongly benefited from such a development because the signal-to-noise ratio (SNR) of the detected dipolar evolution is directly proportional to the fraction of the spins inverted by the so-called pump pulse(s). For example, the pulse-shaping technology could provide up to several-fold gain in SNR in comparison to short approximately rectangular pump pulses in application to spin labels with broad EPR spectra such as, for example, Co^{2+} and Gd^{3+} [34–37].

Further improvements in DEER signal-to-noise ratio have been achieved by implementing decoupling schemes. Specifically, Borbat et al. demonstrated that the dead-time-free 4-pulse DEER sequence can be further optimized by taking into account intrinsic properties of the electron spin phase memory relaxation albeit only for the systems with a significant contribution of nuclear spin diffusion and, unfortunately, at the cost of noticeable experimental artifacts [38]. This idea of using the Carr-Purcell (CP) nuclear spin decoupling scheme [39] for dynamical decoupling of electronic spins [40] provided a further boost for the recent advances in the PDS spectroscopy [41–45].

In spite of the dramatic improvement in DEER sensitivity achieved through this remarkable progress in both instrumentation and/or pulse sequences, measurements of long interspin distances in membrane proteins continue to be challenging. For the latter systems the electronic spin phase memory time may be as short as 0.6 μs [38], thus, limiting the length of a reliably measured DEER trace to just a few microseconds.

We note that nearly all the DEER pulse sequences described in the literature are based on acquiring the experimental signal at fixed positions of the observer pulses. For such pulse sequences the cumulative length of the observer pulse train (*i.e.*, the sum of intervals between all the observer pulses) must be longer than the length of the measured DEER trace. Then for the trace significantly longer than T_m, the DEER signal represents measurements of the amplitude of an extremely damped electron spin echo signal which has a very poor SNR. While such a selection of a weak echo signal as the basis for the measurements seems to be irrational at a first glance, keeping the observer pulse positions fixed allows for the main advantage of DEER spectroscopy – selective detection of electron-electron dipolar interactions. Attempts to improve 4-pulse DEER sensitivity by moving the third observer pulse simultaneously with the pump pulse have been made in the early stages of the PDS development [46]. Although the average SNR has been clearly improved, the disadvantages caused by stepping the observer pulse overweighed the benefits of the improved SNR, thus, preventing the wide use of the proposed method. The disadvantages included the time-dependent noise that was rapidly increasing towards the tail of the trace and eventually exceeding that of the standard 4-pulse DEER as well as artifacts caused by incomplete filtering of the unwanted magnetic interactions.

Here we address the issue of the DEER signal loss due to the fixed positions of the observer pulses. Specifically, we describe a simple but efficient strategy of splitting the DEER trace acquisition into multiple stepwise acquired segments optimally distributed by their length to minimize SNR losses caused by the phase relaxation. Since varying the observer pulse positions has been found to be overall disadvantageous for DEER, each segment is measured with the fixed positions of the observer pulses. By using the standard 4-pulse DEER sequence and two membrane protein complexes as examples, we demonstrate that the proposed DEER with ***REL***axation ***O***ptimized ***A***cquisition (Length) ***D***istribution (DEER-RELOAD) improves SNR without introducing any noticeable artifacts associated with varying the observer pulse positions. We show that splitting DEER trace acquisition into just 2 separate segments may improve SNR by factor of >3, while the sensitivity gain is expected to grow with increasing the number of acquisition segments.

2. Experimental section

2.1. Materials

All chemicals and solvents were purchased from VWR International (Radnor, PA) or MilliporeSigma (Burlington, MA), unless otherwise indicated, and used without further purification. Phospholipids were purchased from Avanti Polar Lipids (Alabaster, AL) as chloroform solutions (>99% pure). (1-Oxyl-2,2,5,5-tetramethyl-Δ3-pyrroline-3-methyl)-methanethiosulfonate (MTSL) was purchased from Toronto Research Chemicals Inc. (Toronto, ON, Canada). 1-Oxyl−2,2,5,5-tetramethyl-2,5-dihydro-1H-pyrrole-3-carboxylic acid (CP) was purchased from Thermo Fisher Scientific

(Waltham, MA). Gramicidin from *Bacillus brevis* was purchased from Fischer Scientific Co. LLC (Pittsburgh, PA), as a mixture of gramicidin A, B, and C.

2.2. Preparation of gramicidin A sample

A mixture of gramicidin A, B, and C containing ~85% of gramicidin A [47] was covalently labeled at the C-terminus with CP spin label based on a literature protocol [48]. After completing the reaction the mixture was diluted with water, the precipitate formed was collected on a filter, washed with 5 ml of water, dried on air, re-dissolved in a mixture $CHCl_3$:CH_3OH (95:5 v/v), and the crude product was separated on a preparative SiliaPlate Extra Hard Layer TLC plate (Silica gel 60 Å F254; SiliCycle Inc., Quebec City, Quebec, Canada) using $CHCl_3$:CH_3OH (95:5 v/v) mixture as an eluent. The band corresponding to the spin-labeled gramicidin A (SL-gA) was verified by mass spectrometry. HRMS (HESI) *m*/*z* calcd for $C_{108}H_{152}N_{21}O_{19}$ $[M + Na]^+$: 2070.14656; found: 2070.14993 $[M + Na]^+$. Mass spectrometry analysis was carried out by a high resolution Thermo Fisher Scientific Extractive Plus MS (Waltham, MA), a benchtop full-scan Orbitrap™ mass spectrometer, using Heated ElectroSpray Ionization (HESI) method. The mass spectrometer was operated in a positive mode.

The peptide was further re-purified on a preparative TLC plate (Silica gel 60 Å F254; Merck KGaA, Darmstadt, Germany) with $CHCl_3$:CH_3OH (95:5 v/v) eluent. SL-gA was reconstituted into multilamellar DMPC (1,2-dimyristoyl-*sn*-glycero-3-phosphorylcholine) lipid bilayers using a literature procedure [48].

2.3. Preparation of Leptosphaeria rhodopsin sample

The expression and purification of *Leptosphaeria* Rhodopsin (LR) were performed as reported previously [49–52]. Briefly, S71C-LR mutant and wild-type LR were expressed in *P. pastoris* strain SMD1168H. The site-direct mutagenesis was performed by Gene Script Ltd. (Piscataway, NJ). The PICZaA vector containing the gene encoding S71C-LR or wild-type LR (both with 6-His tag at the C-terminal) was transformed in *P. pastoris* cells. The cells were initially scaled up in BMD medium (0.5% glucose, 0.4% NH_4Cl, 0.34% yeast nitrogen base, 0.01% biotin, and 100 mM NaH_2PO4, pH 6.0), at 230 rpm and at 30 °C. The cells were collected when the OD_{600} reached 5.0. The collected cells were re-suspended in BMM medium (0.5% methanol, 0.4% NH_4Cl, 0.34% yeast nitrogen base, 0.01% biotin, and 100 mM NaH_2PO_4, pH 6.0) to induce LR expression. The cells were harvested 48 h after induction with addition of all-*trans* retinal to regenerate the expressed opsin.

The harvested cells were digested by lyticase (from *Arthrobacter luteus*, MilliporeSigma) and broken by high-pressure homogenization. The membrane protein was solubilized in 1% Triton X-100, followed by purification using the batch protocol in the Qiagen Ni^{2+}-NTA manual (Qiagen, Mississauga, Ontario, Canada). The final yield of the wild-type and the S71C-LR was ~7 mg per liter of cell culture. Protein concentration was determined by measuring the absorbance of opsin-bound retinal using an extinction coefficient of 48,000 $M^{-1}cm^{-1}$.

The purified S71C-LR was dissolved in a pH 7.5 buffer (50 mM PBS, 100 mM NaCl, 0.05% DDM). The protein was incubated for 1 h at room temperature with a 10-fold molar excess of nitroxide spin labeling reagent, MTSL. The unreacted MTSL was removed by buffer exchange.

The MTSL modified S71C-LR was mixed with the wild type LR (in the same buffer condition) in a molar ratio of 1:10. The protein mixture was reconstituted into liposomes in a protein:lipid ratio of 2.5:1 (w/w). The composition of the liposome was DMPC:DMPA lipids at a 9:1 ratio (w/w). The detergent was removed by Bio-beads (SM-II, Bio-Rad Laboratories, Inc., Hercules, CA). Proteoliposomes were formed and collected by ultracentrifugation at 400,000*g* for one hour. The pellets were collected by ultracentrifuged at 300,000*g*.

2.4. 4-pulse DEER and 4-pulse DEER-RELOAD

A Bruker ELEXSYS E580 spectrometer equipped SuperQFTu bridge, 10 W AmpQ amplifier, and Q-band EN 5107D2 dielectric resonator (Bruker Biospin, Billerica, MA, USA) has been employed for all experiments. The aqueous samples were drawn into Suprasil WG-222 T tubes (o.d. = 1.6 mm, i.d. = 1.1 mm; Wilmad LabGlass, Vineland, NJ, USA), sealed from one end, and then flash-frozen in liquid nitrogen and rapidly transferred into a pre-cooled Q-band resonator. All measurements were carried out at 76 K using a Bruker ER 4118CF flow cryostat cooled by liquid nitrogen. No cryoprotectant was used for DEER measurements.

For DEER experiments (*cf.* Fig. 1) the pump frequency was set 60 MHz higher than the observer frequency and magnetic field was set in order to pump spins at the maximum of the nitroxide spectrum. For all DEER measurements, length of the observer pulse was 12 ns and 20 ns for π/2- and π-pulses respectively. The length of the pump π-pulse was 22 ns. All DEER traces were measured with τ = 160 ns interval between the first and the second observer pulses and 60 ns interval between the second observer and the starting point of the pump pulse. For every scan, each dipolar evolution time point was measured with 200 shots. The shot repetition time was 1000 and 500 μs for DEER experiments with SL-gA and *Leptosphaeria* rhodopsin, respectively. All DEER spectra were acquired with the standard 8-step phase cycling procedure.

For SL-gA, conventional 4-pulse DEER was measured with 60 ns separation between the second observer and the starting position of the pump pulse and 2960 ns separation between the second and third observer pulses. DEER trace was recorded over the length of 4 × 700 ns. The DEER signal was an average of 20 scans.

For DEER-RELOAD with 1 stitch (SL-gA) the first section was measured with 60 ns separation between the second observer and the starting position of the pump pulse and 2280 ns separation between the second and the third observer pulses. DEER trace was recorded over the length of 4 × 535 ns. The signal was an average of 3 scans. The second (last) section was measured with 2160 ns separation between the second observer and the starting position of the pump pulse and 2960 ns separation between the second and the third observer pulses. DEER trace was recorded over the length of 4 × 175 ns. The signal was an average of 20 scans.

For DEER-RELOAD with 2 stitches (SL-gA) the first section was measured with 60 ns separation between the second observer and the starting position of the pump pulse and 1980 ns separation between the second and the third observer pulses. DEER trace was recorded over the length of 4 × 455 ns. Only 1 scan was measured. The second (middle) section was measured with 2020 ns separation between the second observer and the starting position of the pump pulse and 2560 ns separation between the second and the third observer pulses. DEER trace was recorded over the length of 4 × 155 ns. The signal was an average of 6 scans.

The third and the last section was measured with 2620 ns separation between the second observer and the starting position of the pump pulse and 2960 ns separation between the second and the third observer pulses. DEER trace was recorded over the length of 4 × 100 ns. The signal was an average of 20 scans.

For spin-labeled *Leptosphaeria* rhodopsin, 4-pulse DEER was measured with 60 ns separation between the second observer and the starting position of the pump pulse and 4320 ns separation between the second and the third observer pulses. DEER trace was recorded over the length of 4 × 1050 ns. The signal was an average of 552 scans.

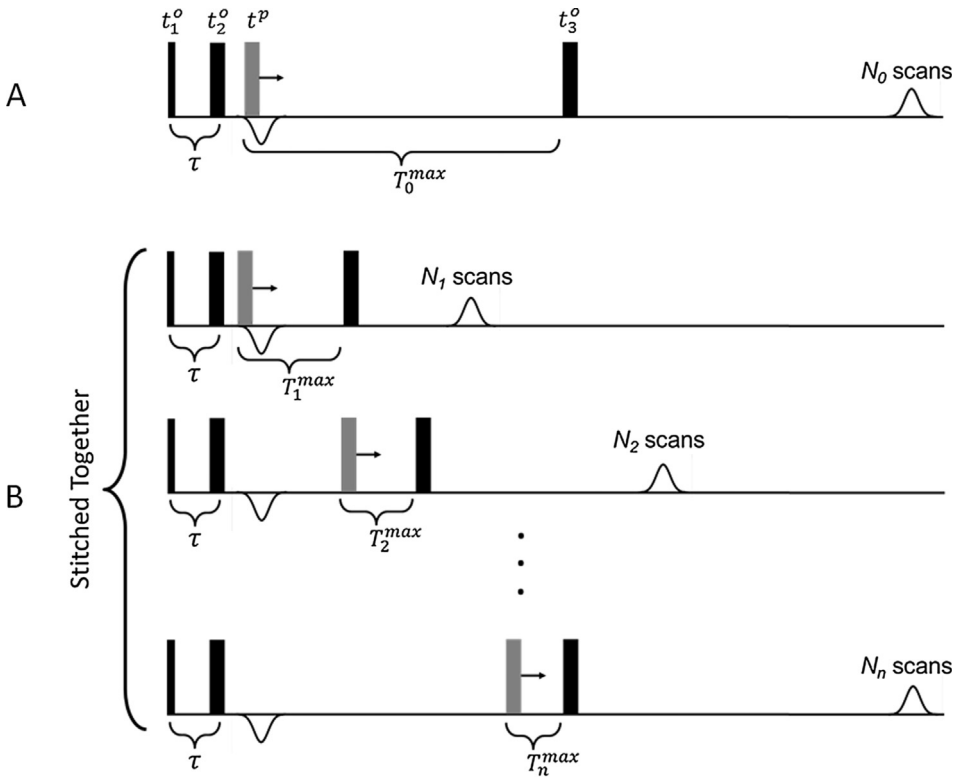

Fig. 1. Pulse sequences and data acquisition schemes for (A) 4-pulse DEER [10] and (B) 4-pulse DEER-RELOAD (see text for description). The observer and the pump pulses are shown as black and grey rectangles, respectively.

For DEER-RELOAD with 1 stitch (*Leptosphaeria* rhodopsin) the first section was measured with 60 ns separation between the second observer and the starting position of the pump pulse and 3360 ns separation between the second and the third observer pulses. DEER trace was recorded over the length of 4 × 800 ns. The signal was an average of 120 scans. The second (last) section was measured with 3160 ns separation between the second observer and the starting position of the pump pulse and 4320 ns separation between the second and the third observer pulses. DEER trace was recorded over the length of 4 × 275 ns. The signal was an average of 1060 scans.

3. Results and discussion

3.1. SNR gain by distributing DEER acquisition

Let us consider how the RELOAD data acquisition scheme reduces the overall time of the DEER experiment while keeping the same SNR. We will discuss the benefits on an example of the most broadly applied 4-pulse DEER sequence [10] while an extension of this strategy to other pulse sequences is rather straightforward.

In 4-pulse DEER, the primary electron spin echo (PE) is formed by the so-called A-spins after the first two $\pi/2$-τ-π pulses are applied at the observer frequency (Fig. 1). The third observer π-pulse is then applied with the delay, T_0^{max}, after the primary echo to generate the secondary refocused echo (RE). Another π pulse at a different (pump) frequency between the second and the third observer pulses flips the so-called B-spins coupled to the A-spins by magnetic dipole-dipole interaction. The position, t^p, of this pump pulse is stepped from slightly before the PE (*i.e.*, in order to measure the zero time region of the DEER trace) to slightly before the third observer pulse (*i.e.*, to prevent the pulse overlap as well to avoid a small "2 + 1" artifact sometimes appearing at the end of a DEER trace). The 4-pulse DEER signal, $V_D(T)$, is recorded as an intensity of the RE *vs*. time separation, T, between the PE and the pump pulse:

$$V_D(T) = V_0 V_{Rel}(2\tau) V_{Rel}(2T_0^{max}) V_{Dip}(T) \quad (1)$$

where V_0 is the intensity of the electron spin echo without accounting for the relaxation damping (*i.e.*, an experimental scaling factor determined by spectrometer configuration, number of spins in the sample, *etc.*), $V_{Rel}(t)$ is the function of the echo damping due to the phase memory relaxation, usually approximated as $\exp\left[-(t/T_m)^k\right]$ [21] with T_m being the phase memory time and k being a parameter determined by relaxation mechanism, and $V_{Dip}(T)$ is the dipolar modulation envelope function representing the normalized DEER signal. For simplicity, let us omit $V_{Dip}(T)$ in the further analysis by assuming $V_{Dip}(T) = 1$.

Let us reasonably assume that the overall acquisition time of the DEER experiment, t_0^{Acq}, is approximately given by a product of the shot repetition time (t_{srt}), number of shots per one point (h), number of points in the DEER trace (N_{tr}) and the number N_0 of the averaged scans because a single DEER trace is recorded by stepping the inter-pulse delay T with the identical number of the repetitions being recorded for the every data point, *i.e.*:

$$t_0^{Acq} \cong t_{srt} h N_{tr} N_0 \quad (2)$$

This equation can be rewritten in an equivalent form:

$$t_0^{Acq} \cong \frac{t_{srt} h}{d_t} d_t N_{tr} N_0 \quad (3)$$

where d_t is the time increment of the acquired DEER trace.

Let us denote as Δ_N an average noise level of a single DEER scan, $\Delta_t = t_{srt} h / d_t$ - single scan acquisition time per unit length of the

DEER trace, and $T_0^{max} = d_t N_{tr}$ – full length of the DEER trace. Then the signal-to-noise ratio, *SNR*, obtained after accumulating N_0 scans is:

$$SNR = \frac{V_0 V_{Rel}(2\tau) V_{Rel}(2T_0^{max})\sqrt{N_0}}{\Delta_N} \cong \frac{V_0 V_{Rel}(2\tau) V_{Rel}(2T_0)\sqrt{t_0^{Acq}/T_0^{max}\Delta_t}}{\Delta_N} \quad (4)$$

Since usually the inter-pulse delay τ can be chosen such that $2\tau \ll T_m$, then the term $V_{Rel}(2\tau) \approx 1$ can be omitted from the analysis and:

$$SNR \approx \frac{V_0 V_{Rel}(2T_0^{max})\sqrt{t_0^{Acq}/T_0^{max}\Delta_t}}{\Delta_N} \quad (5)$$

Alternatively, the acquisition time t_0^{Acq} required for obtaining a certain *SNR* is given by:

$$t_0^{Acq} \approx T_0^{max}\Delta_t\left[\frac{SNR\cdot\Delta_N}{V_0 V_{Rel}(2T_0^{max})}\right]^2 \quad (6)$$

As already discussed in the introduction, in many practical cases experimental DEER signal is measured as amplitude of an extremely damped RE signal, *i.e.*, under conditions when $V_{Rel}(2T_0^{max}) \ll 1$. At a first glance, fixing the position of the third observer pulse for the entire duration of the DEER experiment seems to be irrational, since this pulse is only required to be positioned after the moving pump pulse. Thus, in principle, a fraction of the DEER trace could be acquired using a shorter T_0^{max}, i.e. when the RE intensity is less suppressed. The attractive idea to vary position of the third observer pulse simultaneously with the pump pulse while keeping the minimal separation between them has been tested at the early stages of the DEER method development by Jeschke and coworkers [46]. In their implementation of variable-time DEER all the unwanted signal contributions were suppressed via division by a reference trace, which was measured in the same way but with the pump pulse fixed right at the position of the RE [46]. In spite of yielding an improved SNR on average, this variable-time pulse scheme for DEER did not find a broad use up to this date mainly because of a decreased SNR at the end of the trace and, even more importantly, possible artifacts induced by an incomplete suppression of the unwanted interactions. Thus, keeping the timing of the observer pulses fixed seems to be mandatory in DEER experiments.

We note, however, that fixing the observer pulse positions during the DEER acquisition does not necessary require the entire DEER to be measured with the same positions of the observer pulses. For example, acquiring DEER by using multiple inter-pulse delays τ has been demonstrated to suppress possible electron spin echo envelop modulation (ESEEM) artifacts [46]. More recently, Rein et al. [53] proposed to measure higher and lower frequencies (corresponding to shorter and longer distances, respectively) of the dipolar spectrum separately by multiple (at least two) DEER traces each measured with T_0^{max}, time step d_t and number of scans N_0 optimal for each of the dipolar frequency ranges yielding an overall significantly improved sensitivity in a DEER experiment. Here we propose to acquire the DEER trace stepwise; i.e. the initial trace section $V_1(T)$ of a length T_1^{max} is measured with a short delay T_1^{max} by accumulating N_1 scans. The next section $V_2(T)$ of a length T_2^{max} is measured with a longer delay equal to $T_1^{max} + T_2^{max}$ by accumulating N_2 scans (and so on until the last section $V_n(T)$ of length T_n^{max} is measured by accumulating N_n scans with the longest delay $T_1^{max} + T_2^{max} + \ldots T_n^{max} = T_0^{max}$. Then all the acquired sections (V_1, V_2, … V_n) are "stitched together" yielding a continuous trace $V_{D\text{-}R}$ of the length T_0^{max}. The total number of sections, n, the length of each individual section, T_i^{max}, and number of accumulated scans for each of the sections, N_i, (i = 1, 2, … n) could be optimized to minimize the DEER acquisition time for yielding the same *SNR*. In other words, the acquisition of the entire DEER trace length is distributed in a relaxation-optimized way over the multiple stepwise acquired sections. The scheme of such a DEER experiment with ***REL***axation ***O***ptimized ***A***cquisition ***D***istribution (DEER-RELOAD) is shown in Fig. 1B. For more accurate "stitching", a small overlap δT between each pair of the neighboring sections might be useful. For latter implementation of DEER-RELOAD, a slightly longer trace $T_i^{max} + \delta T$ has to be acquired starting from the second section, (*i.e.*, i = 2, 3… n) in order to provide for a partial overlap. However, as it is shown below such an overlap is not generally required and in the following we will neglect δT, *i.e.* consider only non-overlapping segments.

It should be noted here that the idea of stitching different DEER trace segments has been earlier proposed in the DEER-Stitch method developed by Lovett et al. [54]. The authors suggested improving the overall SNR in a DEER experiment by stitching together a short section of the trace around zero time point acquired using the dead-time-free 4-pulse sequence while the rest of the trace is measured using the 3-pulse sequence. Thus, the dead time distortions are eliminated, while the overall sensitivity is gained from using the shorter 3-pulse train for the rest of the DEER trace [54]. While this DEER-Stich method capitalizes on a greater intensity of the primary echo (PE) of the 3-pulse DEER sequence over the RE employed in the 4-pulse DEER, it requires stitching DEER traces obtained by two different pulse sequences. As was noted by Lovett et al. the 2-pulse echo and 3-pulse refocused echo sequences do not necessarily have exactly the same excitation profiles, therefore, resulting in different modulation depth and orientation selection [54]. Further, the 3-pulse DEER suffers from a dynamic phase shift which must be corrected before digital stitching with the 4-pulse segment [54]. Even more importantly, the timing of the PE is still fixed and is suboptimal in the same way as for 4-pulse DEER experiment discussed above. In other words, the DEER-Stich is essentially a fixed-timing 3-pulse DEER experiment with the initial section corrected by stitching on a dead-time-free 4-pulse DEER segment. The DEER-RELOAD scheme described here could also be applied to 3-pulse DEER and then combined with the initial dead-time-free segment measured with 4-pulse sequence, thus, providing a further sensitivity increase for the DEER-Stitch. This would be one of many possible implementations of DEER-RELOAD.

The DEER-RELOAD scheme offers a flexibility of each individual section being acquired with different increments (*i.e.*, non-uniform sampling between different stitches) and also *SNR*. *SNR*-weighting could be potentially advantageous for the DEER traces with the characteristic features not uniformly distributed over the length. Nevertheless, in all the further discussions we will consider only the case of uniform noise level as the positions of the characteristic features may not be known a priori. Then it can be shown that the total acquisition time of such a DEER-RELOAD trace with uniform noise level and stitched from n segments is given by:

$$t_n^{Acq} \approx \Delta_t\left[\frac{SNR\cdot\Delta_N}{V_0}\right]^2\left\{\frac{T_1^{max}}{\left[V_{Rel}(2T_1^{max})\right]^2} + \frac{T_2^{max}}{\left[V_{Rel}(2T_1^{max}+2T_2^{max})\right]^2} + \ldots\frac{T_n^{max}}{\left[V_{Rel}(2T_0^{max})\right]^2}\right\} \quad (7)$$

Obviously, if $V_{Rel}(t)$ is a monotonous decaying function, then $t_n^{Acq} < t_0^{Acq}$, and DEER-RELOAD pulse scheme would require a shorter acquisition time as compared to the standard DEER for the same *SNR*. Let us now introduce the acquisition time efficiency of the DEER-RELOAD, $\xi_{D\text{-}R}(n)$, defined as:

$$\xi_{\text{D-R}}(n) = \frac{t_0^{\text{Acq}}}{t_n^{\text{Acq}}} = T_0^{\max}\left\{T_1^{\max}\left(\frac{V_{\text{Rel}}(2T_0^{\max})}{V_{\text{Rel}}(2T_1^{\max})}\right)^2 + T_2^{\max}\left(\frac{V_{Rel}(2T_0^{\max})}{V_{\text{Rel}}(2T_1^{\max}+2T_2^{\max})}\right)^2 + \ldots + T_n^{\max}\right\}^{-1} \quad (8)$$

Assuming $V_{\text{Rel}}(t)$ as a stretched exponential function $V_{\text{Rel}}(t) = \exp\left[-(t/T_{\text{m}})^k\right]$, we obtain:

$$\xi_{\text{D-R}}(n) = T_0^{\max}\left\{T_1^{\max}\exp\left[2^{k+1}\left[(T_1^{\max}/T_{\text{m}})^k - (T_0^{\max}/T_{\text{m}})^k\right]\right] + T_2^{\max}\exp\left[2^{k+1}\left[((T_1^{\max}+T_2^{\max})/T_{\text{m}})^k - (T_0^{\max}/T_{\text{m}})^k\right]\right] + \ldots + T_n^{max}\right\}^{-1} \quad (9)$$

For $n \to +\infty$ the sum in Eq. (9) can be approximated by a definite integral yielding:

$$\xi_{\text{D-R}}(+\infty) = \frac{T_0^{\max}\exp\left[2^{k+1}\left[(T_0^{\max}/T_{\text{m}})^k\right]\right]}{\int_0^{T_0^{\max}}\exp\left[2^{k+1}\left[(t/T_{\text{m}})^k\right]\right]dt} \quad (10)$$

Then for the most common case of $k = 1$:

$$\xi_{\text{D-R}}(+\infty) = \frac{4T_0^{\max}}{T_{\text{m}}} \quad (11)$$

From Eq. (11) one could easily see that the savings in the data acquisition time from employing the DEER-RELOAD scheme *vs.* conventional 4-pulse DEER are significant for typical experimental conditions. For example, if one sets $T_0^{\max} = 3T_{\text{m}}$ corresponding to a factor of ≈400 suppression of the RE amplitude, the maximal possible acquisition efficiency of the DEER-RELOAD, $\xi_{\text{D-R}}(+\infty) = 12$ (for $k = 1$).

In practice, however, one has always to choose a realistically small number n of the segments acquired. Nevertheless, even for $n = 2$ or 3 a significant time saving is still achieved. This is illustrated by Fig. 2A which shows the calculated acquisition time efficiency $\xi_{\text{D-R}}(n = 2)$ of DEER-RELOAD acquired as two sections *vs.* the standard 4-pulse DEER for $k = 1$, $T_0^{\max} = 3T_{\text{m}}$ and $k = 1$, $T_0^{\max} = T_{\text{m}}$ as a function of the relative position of the stitch. In these particular examples, an approximately fourfold the gain in the acquisition time efficiency (or 2-fold gain in *SNR*) may be obtained if the DEER acquisition is divided into just two sections with the first one having the length of $\approx 0.8 \cdot T_0^{\max}$ and the second $\approx 0.2 \cdot T_0^{\max}$. Fig. 2B shows how the acquisition efficiency in the same example grows if the number of the segments increases: $\xi_{\text{D-R}}$ grows rapidly for a small number of segments and then exhibits a clear saturation behavior reaching $\xi_{\text{D-R}} \approx 11 - 13$ at $n \to +\infty$.

Eqs. (10) and (11) provide for a comparison of the acquisition efficiencies of DEER-RELOAD *vs.* variable-time DEER [46] assuming that the latter signal could be acquired in a manner to yield a uniform noise distribution. Since in the variable-time DEER an additional reference trace has to be measured as a part of the same experiment, the efficiency $\xi_{\text{D-R}}(+\infty)$ in Eqs. (10) and (11) has to be divided by a factor of 2. Additionally, squared noise levels are added upon the division procedure resulting in an additional factor of 2 loss in the efficiency. Thus, for the particular case of $T_0^{\max} = 3T_{\text{m}}$ and $k = 1$, the acquisition efficiency of the variable-time DEER is equal to 3. This is still measurably lower than the efficiencies of 3.7 and 5.6 predicted for DEER-RELAOD even with just one and two stitches, respectively.

The maximal savings in data acquisition time offered by DEER-RELOAD depend on the RE relaxation damping factor $V_{\text{Rel}}(2T_0^{\max})$: the stronger the damping, the higher the acquisition efficiency of DEER-RELOAD is. Fig. 2C illustrates the dependence of the maximal acquisition efficiency of the DEER-RELOAD with one and two stitches on the stretch exponential parameter $(T_0^{\max}/T_{\text{m}})^k$ for $k = 1, 2$. The efficiency grows nearly linear reaching ~18 for two stitches, $k = 2$, and somewhat unrealistically long DEER trace defined by $(2T_0^{\max}/T_m)^k = 12$.

As another example, Fig. 3 shows how $\xi_{\text{D-R}}$ is distributed over the possible relative positions of the stitches for $n = 3$ segments and $k = 1$, $T_0^{\max} = 3T_{\text{m}}$ and $k = 2$, $T_0^{\max} = T_{\text{m}}$, (Fig. 3A and B, respectively). In both cases, a rather sharp efficiency peak is

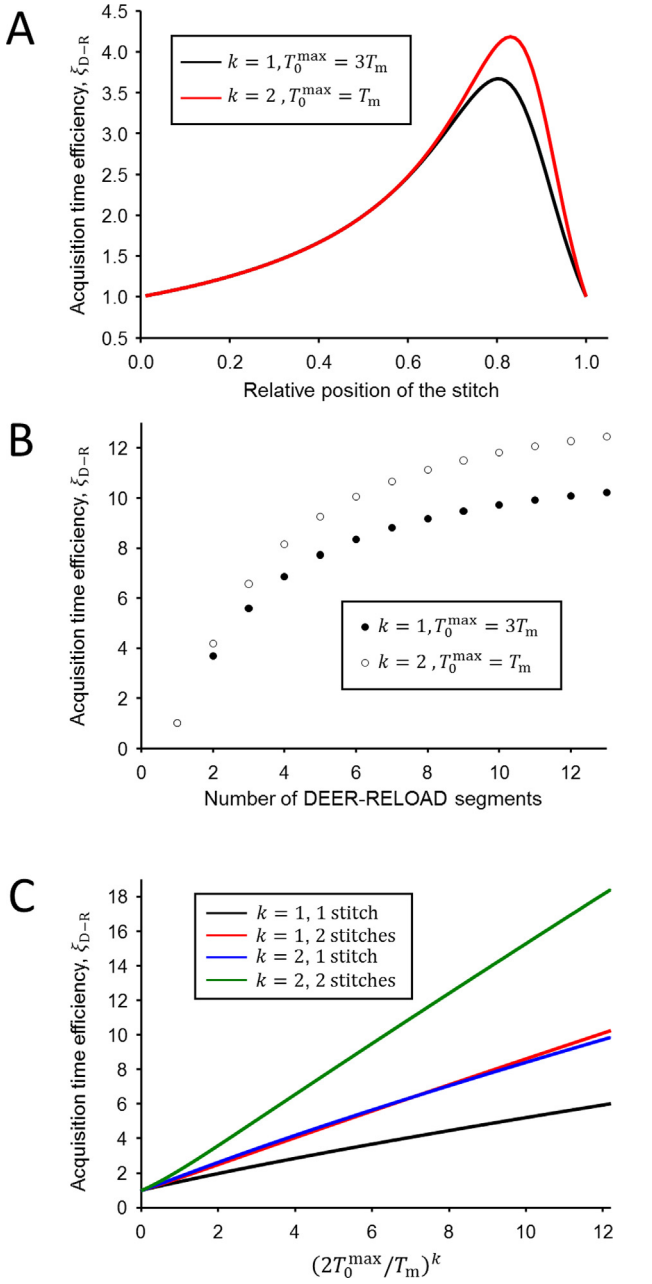

Fig. 2. (A) Calculated DEER-RELOAD acquisition efficiency $\xi_{\text{D-R}}(n = 2)$ as a function of the relative position of the stitch for $k = 1$, $T_0^{\max} = 3T_{\text{m}}$ (black line) and $k = 2$, $T_0^{\max} = T_{\text{m}}$ (red line). (B) Dependence of the calculated DEER-RELOAD acquisition efficiency $\xi_{\text{D-R}}(n)$ on the number of the segments n for $k = 1$, $T_0^{\max} = 3T_{\text{m}}$ (filled circles) and $k = 2$, $T_0^{\max} = T_{\text{m}}$ (open circles). (C) Calculated dependence of the maximal DEER-RELOAD acquisition efficiency $\xi_{\text{D-R}}(n)$ on the stretched exponential parameter $(2T_0^{\max}/T_{\text{m}})^k$ for $n = 2$, $k = 1$ (black line); $n = 2$, $k = 2$ (red line); $n = 3$, $k = 1$ (blue line); and $n = 3$, $k = 2$ (green line). (For interpretation of the references to colour in this figure legend, the reader is referred to the web version of this article.)

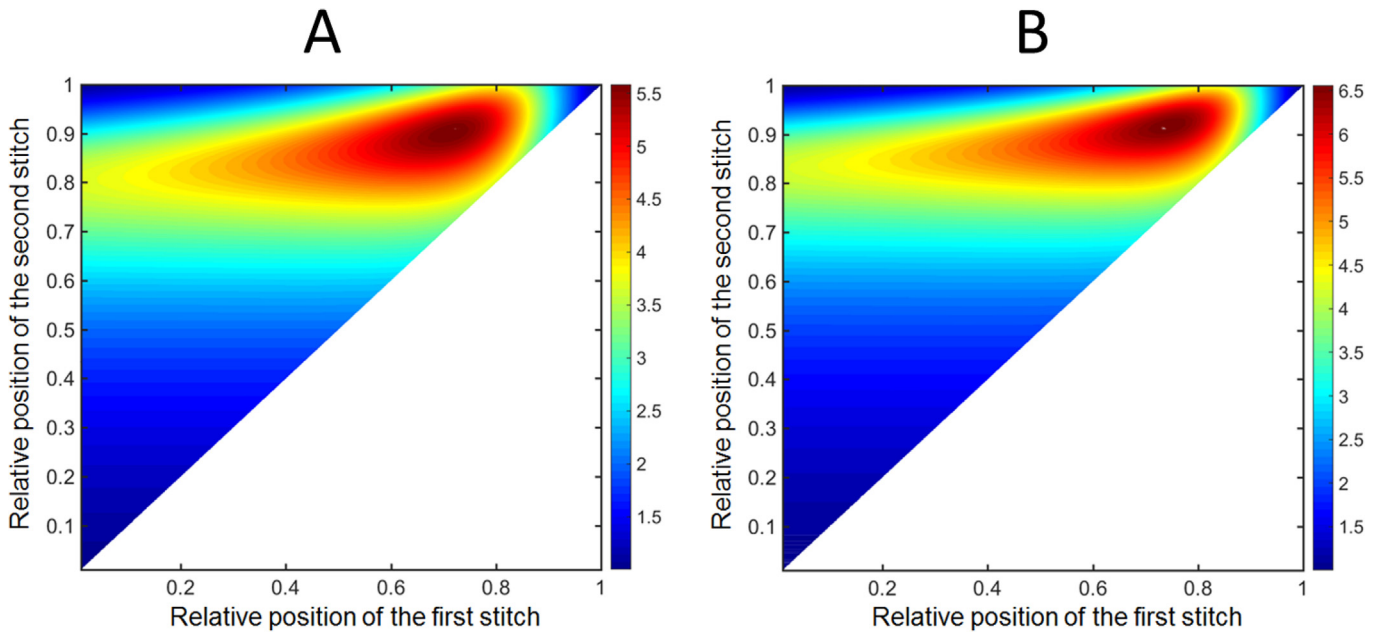

Fig. 3. Contour plots of the calculated DEER-RELOAD acquisition efficiency, $\xi_{\text{D-R}}(3)$, for $n = 3$ segments as the function of relative position of the stitches for $k = 1$, $T_0^{\max} = 3T_{\text{m}}$ (A) and $k = 2$, $T_0^{\max} = T_{\text{m}}$ (B).

located around the optimal positions of two stitches. Thus, optimally distributing DEER trace acquisition over the fixed number of segments is crucial for achieving the maximal benefits of DEER-RELAOD. Notably, in these particular examples the maximum efficiency is achieved when both stitches are positioned in the tail of the DEER trace which is usually dominated by background signal slowly decaying via intermolecular dipolar interactions and, therefore, lacks well-defined oscillatory features. The latter practical consideration simplifies the choice of the stitching procedure described below.

3.2. Stitching the individual DEER-RELOAD segments

The only obvious drawback of the DEER-RELOAD detection scheme is the necessity for additional post-processing of the experimental signal in order to stitch multiple individually acquired segments, V_1, V_2, … V_n, into a single continuous trace $V_{\text{D-R}}$ with minimal distortions. Indeed, different positions of the RE for the individual DEER-RELOAD segments result in their different amplitude scaling factors which have be corrected during the post-processing step. Such a correction can be easily carried out by using the conditions of the DEER trace continuity at least up to the first derivative and considering that experimental data contain some noise. Then the stitching of two segments V_i and V_{i+1} could be accurately completed, for example, by following the steps below:

(1) A stitching range is chosen. The range is defined by two dipolar evolution time points T_i and T_{i+1} in the vicinity of the stitching position T_i^s, so that: $T_i < T_i^s < T_{i+1}$.
(2) A stitching function $f(T, C_1, C_2 \dots C_l)$ having l adjustable parameters is chosen. The simplest stitching function is the first order polynomial (*i.e.*, $f = C_1 + C_2 T$) with the stitching range being sufficiently small to approximate the stitched region as linear. However, since the stitches are most likely to be located in the tail of the DEER trace where its shape is close to an exponential decay, it might be superior to use an exponential decay function, $f = C_1 \exp(-C_2 T)$, and wider stitching ranges.
(3) Conventional least squares criterion, D_S, defined as:

$$D_S = \sum_{V_i} [f(T, C_1, C_2 \dots C_l) - V_i(T)]^2 + \sum_{V_{i+1}} [f(T, C_1, C_2 \dots C_l) - C_{l+1} V_{i+1}(T)]^2 \quad (12)$$

is then used together with one of the standard minimization procedures to yield the best fit parameters $C_1, C_2 \dots C_l$ for the stitching function f as well as an additional stitching parameter C_{l+1}. Here the sums are taken over the points of the two stitched segments within the stitching range.
(4) Ones the stitching parameter, C_{l+1}, is determined from the fitting, the joint $V_{i,i+1}$ segment is constructed as:

$$V_{i,i+1}(t) = \begin{cases} V_i(T) & \text{for } T < T_i^s \text{ and segments do not overlap} \\ \frac{1}{2}(V_i(T) + C_{l+1} V_{i+1}(T)) & \text{for } T \text{ where segments overlap} \\ C_{l+1} V_{i+1}(T) & \text{for } T > T_i^s \text{ and segments do not overlap} \end{cases} \quad (13)$$

An extension of this procedure to more than two segments is straightforward.

Let us now estimate the error introduced by the segment stitching procedure. Assuming a random Gaussian noise characterized by an amplitude Δ_N, total number of data points K_i^s of the two segments contributing to the chi square parameter D_S (Eq. (12)), and also the ideal choice for the fitting function, the error in the stitching parameter C_{l+1}, will be $\approx \Delta_N / \sqrt{K_i^s}$, which is a small fraction of the average noise level in the DEER trace. In practice, however, the error is expected to be somewhat bigger mainly due to non-ideality of the stitching function but the latter could be partially compensated by a proper choice of the stitching range. Ideally, the stitching range should be short enough to be well approximated by an operator-chosen stitching function (*e.g.*, straight line, exponential, higher order polynomial, *etc.*) but also be sufficiently long to provide for a statistically significant number of data points to mitigate effects of the experimental noise during the least-squares fitting (Eq. (12)). Finally, we note that a reasonably

accurate stitching could be even carried out by manually tuning the scaling parameter C_{l+1} to achieve the best visual continuity of the trace. While we strongly recommend using an automated algorithm for the stitching in order to avoid potential subjectivity in the analysis, visual inspection might still be very useful to check for a possible software malfunction.

In contrast to DEER-Stitch experiment [54] in which two trace segments are acquired with two differently designed pulse sequences (which may even have different time scales and require accurate re-phasing of the 3-pulse segment), all the segments of the DEER-RELOAD represent different sections of virtually the same continuous DEER trace. Thus, DEER-RELOAD segments are not required to overlap in any significant way to be accurately stitched together. Unless the total number of segments is large, even small gaps between the segments could be tolerable if the stitches are located at the end of trace where DEER signal undergoes little changes and is well approximated by a low order polynomial or an exponential function. This is in a contrast to the data post-processing of 4- and 3-pulse traces in the DEER-Stitch experiment that requires strongly overlapping segments partially because the stitch position typically falls at the beginning of the trace [54] where the DEER signal undergoes rather rapid changes.

While from a theoretical perspective the sensitivity of DEER-RELOAD should only improve with increasing the number of acquired segments, the practicality of the setting up such a DEER experiment dictates the number of the segments to be reasonably small. Obviously, at some point the distortions introduced by multi-stitching may overweigh the advantages gained by the more efficient data acquisition in terms of *SNR*. As it has been illustrated above for $T_0^{\max} = 3T_m$, the data acquisition efficiency of DEER-RELOAD quickly saturates after *ca.* 4 stitches. Thus, we speculate that distributing the 4-pulse DEER acquisition into 3–5 segments could probably be the best choice, although defining the mathematically rigorous criteria for the optimal number of segments remains an open question.

It is important to note here that the DEER-RELOAD approach is strictly valid only under an assumption of the dipolar modulation envelope function (V_{Dip} in Eq. (1)) being independent of $T_0^{\max}$, *i.e.* the shape of a conventional DEER trace should not change with the position of the last observer pulse. This, however, might be not true if there is phase relaxation dispersion among the observer spins. One example would be provided by a sample with two types of spin pairs each having $T_m^1 \neq T_m^2$. For such systems the distance distribution measured by the conventional DEER might depend on T_0^{max} with distances corresponding to the faster relaxing observer spins being suppressed if T_0^{max} is sufficiently long. The distance distribution measured by DEER-RELOAD in this case might also be distorted, however, in a more complex way than in the case of the conventional DEER and depending on the number and location of the stitches. In the example shown below, a small phase relaxation dispersion of the observer spins results in a significant reduction of the modulation depth observed by conventional 4-pulse DEER, while it could at least partially be recovered by the DEER-RELOAD scheme. In general, if the two spins in a pair have very distinct EPR spectra, V_{Dip} could vary with $T_0^{\max}$ without changing the shape of the form-factor but only change the modulation depth. For such a system conventional 4-pulse DEER approach would still be strictly applicable while DEER-RELOAD could potentially produce some unwanted artifacts. Overall, both conventional 4-pulse DEER and DEER-RELOAD approaches have to be applied with an extra care if any substantial dispersion of the phase memory time takes place among the observer spins.

3.3. Comparison of 4-pulse DEER and DEER-RELOAD in application to membrane protein complexes

Two membrane protein complexes have been chosen for testing (*i*) theoretically predicted sensitivity gain of DEER-RELOAD as compared to the standard 4-pulse DEER and (*ii*) whether any artifacts are generated by the stitching of the individual segments.

3.3.1. "Easy case": gramidicin A in multilamellar DMPC liposomes

Pentadecapeptide gramicidin A from bacterium *Bacillus brevis* is known to form membrane-spanning dimeric ion channels in the bilayers composed of the lipids to provide the proper hydrophobic match [47]. For such a peptide dimer nitroxide spin labels attached to each of the C-terminal ethanolamine groups would form a spin pair with the interspin distance of 3.09 ± 0.05 nm when inserted into DMPC bilayers [48]. This moderately short distance should yield a dipolar modulation with <1 μs period in the DEER trace which can be acquired with a moderate loss of the echo signal due to relaxation damping, V_{Rel}. Experimentally measured $V_{Rel}(t)$ was found to be nearly monoexponential ($k = 1$) with the phase memory time of $T_m = 1.4\mu s$ (not shown). For the DEER trace of $T_0^{\max} = 2.7\mu s$ in length the damping factor of the RE due to the phase relaxation is $V_{Rel} \approx 50$, thus, representing a rather "easy" case for a DEER experiment.

Fig. 4A shows an experimental trace measured at Q-band using the standard 4-pulse DEER by averaging over 6 h 30 min (black line). For a comparison 4-pulse DEER-RELOAD trace obtained using a single stitch at ≈2 μs and averaged over 2 h 20 min (red line) is superimposed on the top of the conventional 4-pulse trace. The traces are virtually identical with the largest deviation at $T \approx 300$ ns most probably due to a random noise not associated with the DEER-RELOAD acquisition scheme. The stitching procedure was performed as described above using an exponential decay stitching function, $C_1\exp[-C_2T]$. The stitching region together with the best fit is shown as an inset (Fig. 4A).

Fig. 4B demonstrates that one could shorten the data acquisition time even further to only 1 h 30 min by employing DEER-RELOAD with two relaxation-optimized stitches and still achieve virtually the same *SNR*. This represents a factor of 4.3 saving in the data acquisition time. Alternatively, one would expect at least 2-fold increase in *SNR* for the same total data acquisition time when using DEER-RELOAD with 2 stitches *vs.* conventional 4-pulse DEER for this membrane protein system. These results provide a clear demonstration of the efficiency of the DEER-RELOAD signal acquisition scheme in terms of *SNR* for the same duration of the DEER experiment (cf. Eq. (8)).

Additional insight on possible artifacts induced by stitching experimental traces in the 4-pulse DEER-RELOAD experiment was obtained by reconstructing the distance distributions for all three experimental DEER traces shown in Fig. 4A and B using DeerAanalysis2015 software [55]. For SL-gA dimer reconstituted in DMPC multilamellar bilayers a uniform two-dimensional distribution was assumed for the background signal and the optimal regularization parameter was set to $\lambda = 100$. The distribution obtained from conventional 4-pulse DEER without any stitches (Fig. 4C, black solid line) revealed no long distance artifacts and a single slightly asymmetric peak at 2.91 ± 0.10 nm which is in agreement with the average distance of 3.09 ± 0.05 nm reported by Dzikovski et al. [48]. The distributions obtained from 4-pulse DEER-RELOAD traces having 1 and 2 stitches (Fig. 4C, red solid and blue dashed lines, respectively) were nearly identical to that of conventional 4-pulse DEER. Only two small deviations were noticeable. Firstly, the main distance distribution peak at 2.91 ± 0.10 nm was subtly distorted by a small broadening.

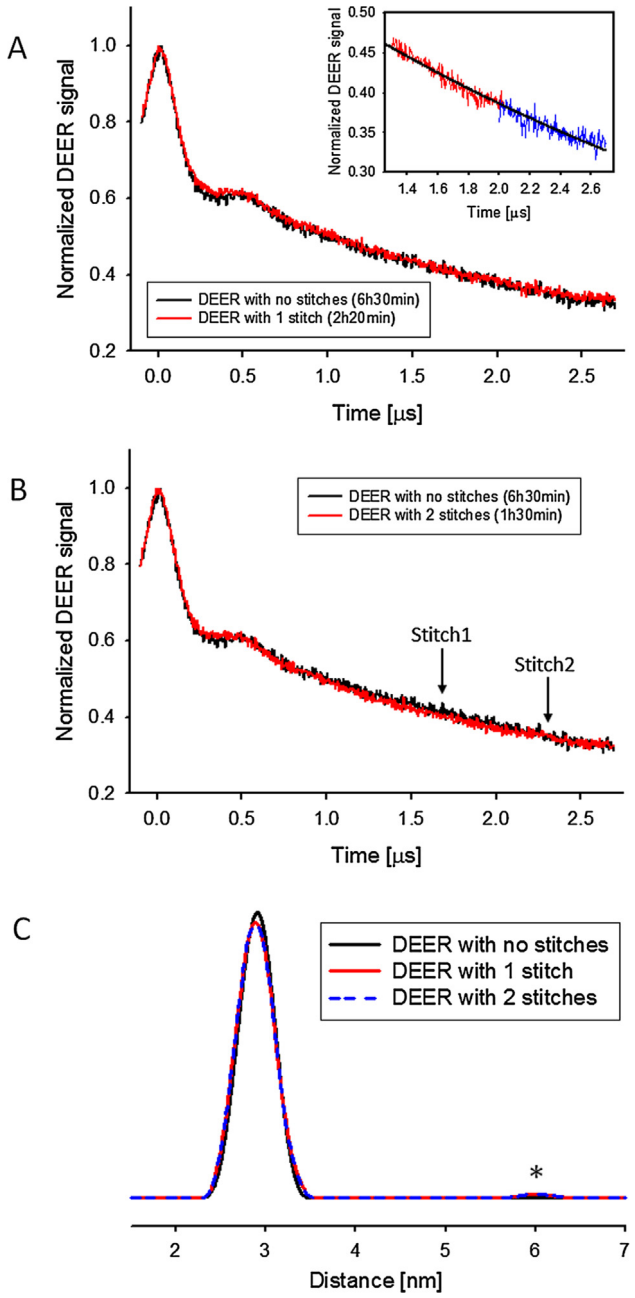

Fig. 4. 4-pulse DEER trace from SL-gA dimer reconstituted in DMPC multilamellar bilayers and averaged over 6 h 30 min (black line in both A and B) is compared with 4-pulse DEER-RELOAD signal (red line) measured as (A) two segments with the total data acquisition time of 2 h 20 min and (B) three segments measured over 1 h 30 min. The inset in (A) shows the results of the least square fitting of the two segments shown as a red and a blue line, respectively, to an exponential stitching function (black line) within the chosen stitching region. (C) Corresponding distance distributions obtained with DeerAanalysis2015 software [55] using optimal regularization parameter $\lambda = 100$ and assuming two-dimensional homogeneous background signal. An asterisk denotes a long distance artifact appearing in 4-pulse DEER-RELOAD that is absent in the conventional 4-pulse DEER. See text for further details. (For interpretation of the references to colour in this figure legend, the reader is referred to the web version of this article.)

Secondly, a small long distance artifact appeared at *ca.* 6 nm (indicated by an asterisk in Fig. 4C). While the small distortion of the main 2.91 ± 0.10 nm peak is likely due to a random noise artifact at ~0.3 μs of the conventional 4-pulse DEER and is not related to stitching, the artifact at *ca.* 6 nm could arise from unwanted "2 + 1" contribution enhanced in the DEER-RELOAD as compared to the conventional DEER. The main reason for the "2 + 1" contribution to become non-negligible is an insufficient 60 MHz separation between the observer and the pump frequencies in both DEER experiments. Thus, in general, the DEER-RELOAD trace has to be acquired with a special care if a partial overlap in the excitation profiles of observer and pump pulses results in characteristic "2 + 1" distortions. While for the conventional 4-pulse DEER it is often sufficient simply to discard the tail of the experimental trace, each of the 4-pulse DEER-RELOAD segments has to be acquired under conditions of a sufficient separation between the pump and the last observer pulses.

3.3.2. "Challenging case": Oligomeric Leptosphaeria rhodopsin in multilamellar DMPC:DMPA liposomes

The second test sample for the efficiency of the DEER-REALOD *vs.* the standard DEER acquisition scheme was provided by *Leptosphaeria* rhodopsin (LR) reconstituted into multilamellar DMPC: DMPA liposomes. LR is a *ca.* 30 kDa eukaryotic rhodopsin from *Leptosphaeria maculans* that in lipid bilayer membranes adapts typical for rhodopsins heptahelical topology. LR is a light-driven proton pump representing a high-performance and extremely versatile class of 'optogenetic' voltage and ion modulators [56]. For DEER experiments, S71C mutant of LR (S71C-LR) was labeled with MTSL. Currently, the structure of LR oligomers is not known but initial chemical cross-linking and light scattering experiments for LR solubilized in a detergent are indicative of a trimer formation [57].

Similar to the methods described by Milikisiyants et al. [23] local concentration of spin-labeled LR oligomers that are expected to form in lipid bilayer membranes was reduced by a diamagnetic dilution with a wild-type LR in 1:10 ratio. Fig. 5A shows the experimental dependence of the refocused echo (RE) intensity for spin-labeled S71C mutant of LR reconstituted in multilamellar DMPC: DMPA liposomes on the delay between the second and third observer pulses (black line) and the best fit to a monoexponential function (dashed red line). Similar to SL-gA dimer, the decay of RE intensity for LR is nearly monoexponential albeit with a significantly shorter $T_m \approx 1.0$ μs. At the very tail of the RE decay (Fig. 5A) the fit yields a longer T_m, thus, indicating some phase memory time anisotropy. Given such a short phase memory time and an expected interspin distance >5 nm, this particular membrane protein sample is particularly challenging to study by DEER spectroscopy. For $T_0^{max} = 4.2$ μs the experimentally measured RE damping factor was ≈2000, thus, requiring very long DEER acquisition time in order to achieve an acceptable *SNR*. Fig. 5B shows the form factor of the DEER trace acquired using the standard 4-pulse sequence (black line) after 5 days of averaging with the inset showing the uncorrected DEER signal (also black line). The trace has still a rather poor *SNR* and the observed shape corresponds to a broadly distributed distance around ≈5.5 nm (reconstructed distance distribution is not shown). For a comparison, the 4-pulse DEER-RELOAD trace measured with one stitch at ≈3 μs and acquired over slightly less than 4 days (red lines in Fig. 5B and insert) has *SNR* exceeding that of the original trace by a factor of ≈2.9. This gain in *SNR* exceeds the factor of 2 predicted by Eq. (8). Although not completely clear, we speculate that this additional *SNR* gain for the DEER-RELOAD trace is at least partially attributed to re-tuning the EPR spectrometer when acquiring shorter individual segments whereas the conventional 4-pulse DEER trace was averaged continuously over a 5-day period and could suffer from phase instability and associated noise. Indeed, a comparison of the signals normalized per one scan of the standard 4-pulse DEER and the second segment of the DEER-RELOAD (not shown) allowed us to estimate the losses due to an increased phase instability as ≈1.23. The authors do not know whether the

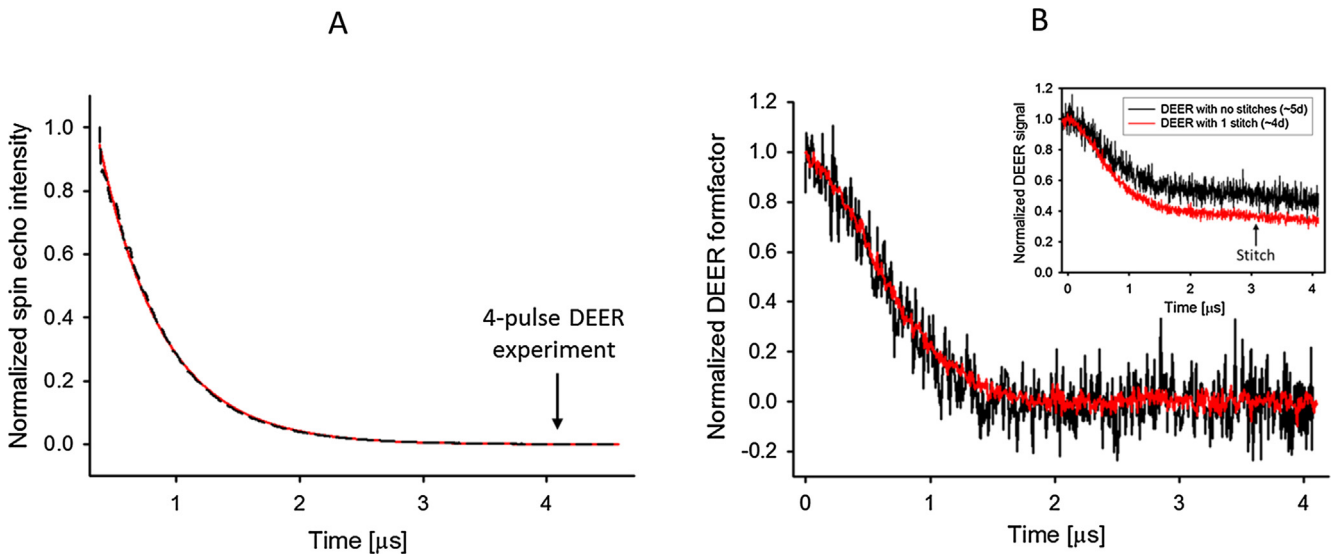

Fig. 5. (A) Experimental dependence of the refocused echo (RE) intensity for spin-labeled S71C mutant of LR reconstituted in multilamellar DMPC:DMPA liposomes on the delay between the second and third observer pulses (black line) and the best fit to a monoexponential function (dashed red line). No DEER pump pulse was applied. Position of the RE for the conventional 4-pulse DEER experiment is indicated by an arrow. (B) Comparison of the form factors extracted from the DEER traces acquired using conventional 4-pulse sequence (black line) by averaging over 5 days and the DEER-RELOAD trace with 1 stitch (red line) acquired over 4 days. The inset shows the DEER and DEER-RELOAD traces before background correction with the stitch position indicated by an arrow. See text for details. (For interpretation of the references to colour in this figure legend, the reader is referred to the web version of this article.)

increased phase instability is associated with a longer trace/time acquisition of the standard DEER (both in length and in time) or it is a pure coincidence. However, we note that any long DEER experiments has increased chances of signal distortions due unpredicted factors related to instrumentation that may also include temperature instabilities, ice buildup in the cryostat due to a slow vacuum leak among many others.

Another clearly noticeable difference between the traces obtained for LR using the standard 4-pulse DEER and 4-pulse DEER-RELOAD sequences is the nearly 1.4-fold larger modulation depth (41% *vs*. 58%) of the singly stitched trace. The modulation depth obtained with DEER-RELOAD (58%) was about double of that obtained SL-gA dimer (30%) and its value is in line with the formation of LR trimers assuming a nearly complete LR labelling efficiency. However, the observed modulation depth in the standard DEER trace is somewhat between the values expected for a dimer (too high) and a trimer (too low). Smaller modulation depth of the standard DEER indicates a loss of structural information that could be at least partially recovered with DEER-RELOAD. The standard DEER trace also appears to be too noisy for an accurate comparison of the modulation depths. One plausible explanation of a lower modulation depth in the standard DEER trace is related to the phase memory time anisotropy mentioned above. Indeed, a fraction of the observer A-spins may have no partnering B-spins in the trimer and, thus, relax slower. The relaxation damping factor for these A-spins is smaller than that of those A-spins in the completely labelled trimers. Since the standard DEER is measured with longer observer inter-pulse delay than the first segment of the DEER-RELOAD trace, the relative contribution of the fully labelled fraction drops further for the standard DEER *vs*. DEER-RELOAD. The magnitude of the drop depends on both the labelling efficiency and a difference in the relaxation rates of the two fractions. Indeed, a 1.4-fold drop over the last ≈1 μs of the $T_0^{max} = 4.2$ μs trace seems reasonable if the partially labeled fraction is small and the difference in the relaxation rates is significant. We note, that similar effects have been recently reported by Baber et al. [58] who observed significant distortions of a DEER trace if T_0^{max} is sufficiently long to suppress the RE signal from the faster relaxing fractions of A-spins.

We note that if a standard 4-pulse DEER trace is distorted by phase relaxation anisotropy, then in DEER-RELAOD experiment the mostly distorted last segment $V_n(T)$ is stitched with a less distorted $V_{n-1}(T)$ segment and then with even lesser distorted $V_{n-2}(T)$ and so on. We speculate that such a signal stitching should lead to at least a partial recovery of the structural information lost in the standard DEER experiment, although the stitching of the segments from slightly differently shaped traces might, in principle, cause some undesired artifacts. In the particular example of S71C-LR shown in Fig. 5, the stitching takes place in the tail region of the trace where the intra-molecular dipolar modulations are nearly completely vanished through dipolar dephasing caused by a relatively broad distance distribution. The shape of the tail of the DEER trace is dominated by intermolecular decay which is similar for all the fractions of the A-spins (assuming the same local spin concentration). Thus, the stitching should not cause any significant distortions of the DEER-RELOAD trace while still providing for a higher modulation depth. Unfortunately, any detailed and/or accurate comparisons of the shapes of the standard DEER and DEER-RELOAD traces for this spin-labeled LR sample are impossible because of a poor *SNR* of the standard DEER trace.

Fig. 5B overlays form factors extracted from the experimental conventional 4-pulse DEER and DEER-RELOAD traces (Fig. 5B insert) using DeerAnalysis2015 software package (see also Ref. [55]). The *SNR* gain for background-corrected data increased to ≈4 because of the enhanced modulation depth. If we discount for a lower detection phase instability discussed above, applying the DEER-RELAOD acquisition scheme for this particular spin-labeled membrane protein resulted in *SNR* enhancement by factor >3 even though the total acquisition time was actually somewhat shorter as compared to the standard DEER. This is significant because achieving the same *SNR* with conventional 4-pulse DEER data acquisition scheme using the same instrument would require signal averaging for >45 days (!).

4. Conclusions

Significant improvement of sensitivity of DEER spectroscopy has been demonstrated by applying the novel ***REL***axation ***O***ptimized ***A***cquisition ***D***istribution (DEER-RELOAD) acquisition scheme to two different spin-labeled membrane protein complexes: an ion channel forming gramicidin A reconstituted into DMPC liposomes and *Leptosphaeria* Rhodopsin in DMPC:DMPA liposomes. The principal advantage of the DEER-RELOAD scheme in terms of the signal-to-noise ratio arises from acquiring a series of the individual segments, which lengths are optimized according the phase memory relaxation profile of the observed A-spins. The segments are stitched together to yield the final continuous trace that is further processed and analyzed in a standard fashion. No artifacts above the average noise level associated with the new acquisition scheme have been observed experimentally. While for spin-labeled gramicidin A, the *SNR* gains were close to those predicted theoretically, an additional factor of ≈1.4 in *SNR* was obtained for *Leptosphaeria* Rhodopsin due to an unexpected increase of the intra-molecular dipolar modulation depth. Enhanced sensitivity of DEER-RELOAD makes it a useful addition to the available methods to measure nm-scale distances in disordered samples and membrane proteins and membrane protein complexes in particular, where the losses in the refocused echo amplitude caused by exceptionally short electron spin phase relaxation are often imposing the critical limitations on the applicability of DEER spectroscopy.

The user-friendly Matlab-based software package StitchFit developed for automated stitching of multiple DEER-RELOD segments into one continuous DEER trace is available for free download using the following link: https://smirnovgroup.wordpress.ncsu.edu/downloads/.

Acknowledgments

We thank U.S. Department of Energy Basic Biosciences Program (DOE Contract DE-FG02-02ER15354) for financial support of DEER method development and grA studies. EPR instrumentation was supported by grants from the National Institutes of Health (no. RR023614), the National Science Foundation (no. CHE-0840501), and North Carolina Biotechnology Center (NCBC no. 2009-IDG-1015). M. A. V. is thankful to NSF (CBET-1403871) for partial financial support. The work on *Leptosphaeria* rhodopsin was supported by the National Key Research and Development Program of the Ministry of Science and Technology of the People's Republic of China (contract number 2016YFA0501203), the National Natural Science Foundation of China (31470727, 21874004), the interdisciplinary medicine Seed Fund of Peking University, and the Beijing National Laboratory for Molecular Sciences, People's Republic of China. Mass spectrometry measurements were carried out in the Molecular Education, Technology, and Research Innovation Center (METRIC) at NC State University.

References

[1] G. Jeschke, Y. Polyhach, Distance measurements on spin-labelled biomacromolecules by pulsed electron paramagnetic resonance, Phys. Chem. Chem. Phys. 9 (2007) 1895–1910.
[2] G. Jeschke, DEER distance measurements on proteins, Annu. Rev. Phys. Chem. 63 (2012) 419–446.
[3] I. Krstic, B. Endeward, D. Margraf, A. Marko, T.F. Prisner, Structure and dynamics of nucleic acids, in: M. Drescher, G. Jeschke (Eds.), EPR Spectroscopy: Applications in Chemistry and Biology, Springer-Verlag Berlin, Berlin, 2012, pp. 159–198.
[4] P.P. Borbat, J.H. Freed, Pulse dipolar electron spin resonance: distance measurements, in: C.R. Timmel, J.R. Harmer (Eds.), Structural Information from Spin-Labels and Intrinsic Paramagnetic Centres in the Biosciences, Springer Berlin Heidelberg, Berlin, Heidelberg, 2013, pp. 1–82.
[5] P.P. Borbat, J.H. Freed, Multiple-quantum ESR and distance measurements, Chem. Phys. Letts. 313 (1999) 145–154.
[6] P.P. Borbat, A.J. Costa-Filho, K.A. Earle, J.K. Moscicki, J.H. Freed, Electron spin resonance in studies of membranes and proteins, Science 291 (2000) 266–269.
[7] P.P. Borbat, J.H. Freed, Double-quantum ESR and distance measurements, in: L. J. Berliner, G.R. Eaton, S.S. Eaton (Eds.), Distance Measurements in Biological Systems by EPR, Springer US, Boston, MA, 2002, pp. 383–459.
[8] A. Milov, K. Salikhov, M. Shirov, Use of the double resonance in electron spin echo method for the study of paramagnetic center spatial distribution in solids, Fizika Tverdogo Tela 23 (1981) 975–982.
[9] A.D. Milov, A.B. Ponomarev, Y.D. Tsvetkov, Electron-electron double resonance in electron spin echo: model biradical systems and the sensitized photolysis of decalin, Chem. Phys. Lett. 110 (1984) 67–72.
[10] M. Pannier, S. Veit, A. Godt, G. Jeschke, H.W. Spiess, Dead-time free measurement of dipole-dipole interactions between electron spins, J. Magn. Reson. 142 (2000) 331–340.
[11] L.V. Kulik, S.A. Dzuba, I.A. Grigoryev, Y.D. Tsvetkov, Electron dipole-dipole interaction in ESEEM of nitroxide biradicals, Chem. Phys. Lett. 343 (2001) 315–324.
[12] Y.M. Abramov, A.M. Vasiliev, V.A. Khlebnikov, R.N. Vasilenko, N.L. Kulikova, I.V. Kosarev, A.T. Ishchenko, J.R. Gillespie, I.S. Millett, A.L. Fink, V.N. Uversky, Structural and functional properties of Yersinia pestis Caf1 capsular antigen and their possible role in fulminant development of primary pneumonic plague, J. Proteome Res. 1 (2002) 307–315.
[13] S. Milikisyants, F. Scarpelli, M.G. Finiguerra, M. Ubbink, M. Huber, A pulsed EPR method to determine distances between paramagnetic centers with strong spectral anisotropy and radicals: the dead-time free RIDME sequence, J. Magn. Reson. 201 (2009) 48–56.
[14] A.A. Kuzhelev, O.A. Krumkacheva, G.Y. Shevelev, M. Yulikov, M.V. Fedin, E.G. Bagryanskaya, Room-temperature distance measurements using RIDME and the orthogonal spin labels trityl/nitroxide, Phys. Chem. Chem. Phys. 20 (2018) 10224–10230.
[15] D. Abdullin, F. Duthie, A. Meyer, E.S. Müller, G. Hagelueken, O. Schiemann, Comparison of PELDOR and RIDME for distance measurements between nitroxides and low-spin Fe(III) Ions, J. Phys. Chem. B 119 (2015) 13534–13542.
[16] A. Doll, M. Qi, A. Godt, G. Jeschke, CIDME: short distances measured with long chirp pulses, J. Magn. Reson. 273 (2016) 73–82.
[17] G. Jeschke, M. Pannier, A. Godt, H.W. Spiess, Dipolar spectroscopy and spin alignment in electron paramagnetic resonance, Chem. Phys. Lett. 331 (2000) 243–252.
[18] V.V. Kurshev, A.M. Raitsimring, Y.D. Tsvetkov, Selection of dipolar interaction by the 2 + 1 pulse train ESE, J. Magn. Reson. 81 (1989) 441–454.
[19] C. Hintze, D. Bücker, S. Domingo Köhler, G. Jeschke, M. Drescher, Laser-induced magnetic dipole spectroscopy, J. Phys. Chem. Lett. 7 (2016) 2204–2209.
[20] E. Bordignon, S. Bleicken, New limits of sensitivity of site-directed spin labeling electron paramagnetic resonance for membrane proteins, Biochimica et Biophysica Acta (BBA) - Biomembranes 1860 (2018) 841–853.
[21] M. Lindgren, G.R. Eaton, S.S. Eaton, B.H. Jonsson, P. Hammarstrom, M. Svensson, U. Carlsson, Electron spin echo decay as a probe of aminoxyl environment in spin-labeled mutants of human carbonic anhydrase II, J. Chem. Soc.-Perkin Trans. 2 (1997) 2549–2554.
[22] M. Huber, M. Lindgren, P. Hammarström, L.G. Mårtensson, U. Carlsson, G.R. Eaton, S.S. Eaton, Phase memory relaxation times of spin labels in human carbonic anhydrase II: pulsed EPR to determine spin label location, Biophys. Chem. 94 (2001) 245–256.
[23] S. Milikisiyants, S. Wang, R.A. Munro, M. Donohue, M.E. Ward, D. Bolton, L.S. Brown, T.I. Smirnova, V. Ladizhansky, A.I. Smirnov, Oligomeric structure of anabaena sensory rhodopsin in a lipid bilayer environment by combining solid-state NMR and long-range DEER constraints, J. Mol. Biol. 429 (2017) 1903–1920.
[24] P.P. Borbat, R.H. Crepeau, J.H. Freed, Multifrequency two-dimensional Fourier transform ESR: an X/Ku-band spectrometer, J. Magn. Reson. 127 (1997) 155–167.
[25] P.A.S. Cruickshank, D.R. Bolton, D.A. Robertson, R.I. Hunter, R.J. Wylde, G.M. Smith, A kilowatt pulsed 94 GHz electron paramagnetic resonance spectrometer with high concentration sensitivity, high instantaneous bandwidth, and low dead time, Rev. Sci. Instrum. 80 (2009).
[26] P. Zou, H.S. McHaourab, Increased sensitivity and extended range of distance measurements in spin-labeled membrane proteins: Q-band double electron-electron resonance and nanoscale bilayers, Biophys. J. 98 (2010) L18–L20.
[27] Y. Polyhach, E. Bordignon, R. Tschaggelar, S. Gandra, A. Godt, G. Jeschke, High sensitivity and versatility of the DEER experiment on nitroxide radical pairs at Q-band frequencies, Phys. Chem. Chem. Phys. 14 (2012) 10762–10773.
[28] C.L. Motion, J.E. Lovett, S. Bell, S.L. Cassidy, P.A.S. Cruickshank, D.R. Bolton, R.I. Hunter, H. El Mkami, S. Van Doorslaer, G.M. Smith, DEER sensitivity between iron centers and nitroxides in heme-containing proteins improves dramatically using broadband, High-Field EPR, J. Phys. Chem. Lett. 7 (2016) 1411–1415.
[29] M. Tseitlin, R.W. Quine, G.A. Rinard, S.S. Eaton, G.R. Eaton, Digital EPR with an arbitrary waveform generator and direct detection at the carrier frequency, J. Magn. Reson. 213 (2011) 119–125.
[30] P.E. Spindler, Y. Zhang, B. Endeward, N. Gershernzon, T.E. Skinner, S.J. Glaser, T. F. Prisner, Shaped optimal control pulses for increased excitation bandwidth in EPR, J. Magn. Reson. 218 (2012) 49–58.
[31] G.B. Park, R.W. Field, Perspective: the first ten years of broadband chirped pulse Fourier transform microwave spectroscopy, J. Chem. Phys. 144 (2016).

[32] A. Doll, G. Jeschke, Wideband frequency-swept excitation in pulsed EPR spectroscopy, J. Magn. Reson. 280 (2017) 46–62.
[33] I. Kaminker, R. Barnes, S. Han, Arbitrary waveform modulated pulse EPR at 200 GHz, J. Magn. Reson. 279 (2017) 81–90.
[34] A. Doll, S. Pribitzer, R. Tschaggelar, G. Jeschke, Adiabatic and fast passage ultra-wideband inversion in pulsed EPR, J. Magn. Reson. 230 (2013) 27–39.
[35] P.E. Spindler, S.J. Glaser, T.E. Skinner, T.F. Prisner, Broadband inversion PELDOR spectroscopy with partially adiabatic shaped pulses, Angewandte Chemie-Int. Ed. 52 (2013) 3425–3429.
[36] A. Doll, M. Qi, N. Wili, S. Pribitzer, A. Godt, G. Jeschke, Gd(III)–Gd(III) distance measurements with chirp pump pulses, J. Magn. Reson. 259 (2015) 153–162.
[37] A. Doll, M.A. Qi, S. Pribitzer, N. Wili, M. Yulikov, A. Godt, G. Jeschke, Sensitivity enhancement by population transfer in Gd(III) spin labels, Phys. Chem. Chem. Phys. 17 (2015) 7334–7344.
[38] P.P. Borbat, E.R. Georgieva, J.H. Freed, Improved sensitivity for long-distance measurements in biomolecules: five-pulse double electron-electron resonance, J. Phys. Chem. Lett. 4 (2013) 170–175.
[39] H.Y. Carr, E.M. Purcell, Effects of diffusion on free precession in NMR experiments, Phys. Rev. 94 (1954) 630–638.
[40] J. Du, X. Rong, N. Zhao, Y. Wang, J. Yang, R.B. Liu, Preserving electron spin coherence in solids by optimal dynamical decoupling, Nature 461 (2009) 1265.
[41] F. Mentink-Vigier, A. Collauto, A. Feintuch, I. Kaminker, V.T. Le, D. Goldfarb, Increasing sensitivity of pulse EPR experiments using echo train detection schemes, J. Magn. Reson. 236 (2013) 117–125.
[42] P.E. Spindler, I. Waclawska, B. Endeward, J. Plackrneyer, C. Ziegler, T.F. Prisner, Carr-Purcell pulsed electron double resonance with shaped inversion pulses, J. Phys. Chem. Lett. 6 (2015) 4331–4335.
[43] C.E. Tait, S. Stoll, Coherent pump pulses in Double Electron Resonance spectroscopy, Phys. Chem. Chem. Phys. 18 (2016) 18470–18485.
[44] A. Doll, G. Jeschke, Double electron-electron resonance with multiple non-selective chirp refocusing, Phys. Chem. Chem. Phys. 19 (2017) 1039–1053.
[45] J. Soetbeer, M. Hulsmann, A. Godt, Y. Polyhach, G. Jeschke, Dynamical decoupling of nitroxides in o-terphenyl: a study of temperature, deuteration and concentration effects, Phys. Chem. Chem. Phys. 20 (2018) 1615–1628.
[46] G. Jeschke, A. Bender, H. Paulsen, H. Zimmermann, A. Godt, Sensitivity enhancement in pulse EPR distance measurements, J. Magn. Reson. 169 (2004) 1–12.
[47] D.A. Kelkar, A. Chattopadhyay, The gramicidin ion channel: a model membrane protein, Biochimica Et Biophysica Acta-Biomembranes 1768 (2007) 2011–2025.
[48] B.G. Dzikovski, P.P. Borbat, J.H. Freed, Spin-labeled gramicidin a: channel formation and dissociation, Biophys. J. 87 (2004) 3504–3517.
[49] S.A. Waschuk, A.G. Bezerra, L. Shi, L.S. Brown, Leptosphaeria rhodopsin: bacteriorhodopsin-like proton pump from a eukaryote, Proc. Natl. Acad. Sci. USA 102 (2005) 6879–6883.
[50] Y. Fan, S. Emami, R. Munro, V. Ladizhansky, L.S. Brown, Isotope labeling of eukaryotic membrane proteins in yeast for solid-state NMR, in: Z. Kelman (Ed.), Isotope Labeling of Biomolecules - Labeling Methods, 2015, pp. 193–212.
[51] J. Liu, C. Liu, Y. Fan, R.A. Munro, V. Ladizhansky, L.S. Brown, S.L. Wang, Sparse C-13 labelling for solid-state NMR studies of *P. pastoris* expressed eukaryotic seven-transmembrane proteins, J. Biomol. NMR 65 (2016) 7–13.
[52] C. Liu, J. Liu, X.J. Xu, S.Q. Xiang, S.L. Wang, Gd^{3+}-chelated lipid accelerates solid-state NMR spectroscopy of seven-transmembrane proteins, J. Biomol. NMR 68 (2017) 203–214.
[53] S. Rein, P. Lewe, S.L. Andrade, S. Kacprzak, S. Weber, Global analysis of complex PELDOR time traces, J. Magn. Reson. 295 (2018) 17–26.
[54] J.E. Lovett, B.W. Lovett, J. Harmer, DEER-stitch: combining three- and four-pulse DEER measurements for high sensitivity, deadtime free data, J. Magn. Reson. 223 (2012) 98–106.
[55] G. Jeschke, V. Chechik, P. Ionita, A. Godt, H. Zimmermann, J. Banham, C.R. Timmel, D. Hilger, H. Jung, DeerAnalysis2006 - a comprehensive software package for analyzing pulsed ELDOR data, Appl. Magn. Reson. 30 (2006) 473–498.
[56] B.Y. Chow, X. Han, A.S. Dobry, X. Qian, A.S. Chuong, M. Li, M.A. Henninger, G.M. Belfort, Y. Lin, P.E. Monahan, E.S. Boyden, High-performance genetically targetable optical neural silencing by light-driven proton pumps, Nature 463 (2010) 98.
[57] L.L. Ji, B.F. Ma, Q. Meng, L.J. Li, K. Liu, D.L. Chen, Detergent-resistant oligomeric *Leptosphaeria* rhodopsin is a promising bio-nanomaterial and an alternative to bacteriorhodopsin, Biochem. Biophys. Res. Commun. 493 (2017) 352–357.
[58] J.L. Baber, J.M. Louis, G.M. Clore, Dependence of distance distributions derived from double electron-electron resonance pulsed epr spectroscopy on pulse-sequence time, Angewandte Chemie-Int. Ed. 54 (2015) 5336–5339.